2021

Preparation and characterization of alginate-b-PLA hydrogels

BOSTON UNIVERSITY

COLLEGE OF ENGINEERING

Thesis

PREPARATION AND CHARACTERIZATION OF ALGINATE-b-PLA HYDROGELS

by

HAOYI HOU

B.E., Zhengzhou University, 2019

Submitted in partial fulfillment of the

requirements for the degree of

Master of Science

2021

Approved by

First Reader

Arturo Vegas, Ph.D.
Assistant Professor of Chemistry
Assistant Professor of Biomedical Engineering
Assistant Professor of Materials Science and Engineering

Second Reader

Mark W. Grinstaff, Ph.D.
Distinguished Professor of Translational Research
Professor of Biomedical Engineering
Professor of Chemistry
Professor of Materials Science and Engineering
Professor of Medicine

Third Reader

Timothy M. O'Shea, Ph.D.
Assistant Professor of Biomedical Engineering

ACKNOWLEDGMENTS

First and foremost I am extremely grateful to my supervisor, Prof. Arturo Vegas for giving me this opportunity to work on this project, continuous support, and patience during my study. I would also like to thank Dr. Yunpeng Feng for his technical support and patient guidance on my study. I would like to thank all the students in Vegas Lab and Professors in my thesis committee. It is their kind help and support that have made my study and life here a wonderful time. Finally, I would like to express my gratitude to my parents and friends. Without their tremendous understanding and encouragement in the past 2 years, it would be impossible for me to complete my study.

PREPARATION AND CHARACTERIZATION OF

ALGINATE-b-PLA HYDROGELS

HAOYI HOU

ABSTRACT

Alginate is a widely used biomaterial for a variety of biomedical applications ranging from drug delivery to cell transplantation. The unique polysaccharide backbone endows the material with a number of useful properties such as hydrophilicity, biocompatibility, and gelation ability. Despite these advantages, one limitation for alginate is the lack of a tunable degradation rate, and its gels may only partially degrade and implants are not fully cleared from the body long after their purpose is fulfilled. To further extend the utility of this biomaterial, we hypothesized that creating a polymer chimera between polylactic acid (PLA) and alginate we can integrate tunable degradation properties into alginate hydrogels. The alginate-*b*-PLA diblock copolymers were synthesized by utilizing an inverse electron demand Diels-Alder reaction, and were then fabricated into hydrogels using two approaches: doping with low viscosity alginate (LWA) and direct gelation. These hydrogel chimeras exhibited degradation rates that could be tuned from days to weeks. Morphologically, the combination of different domain sizes of alginate and PLA contributed to different microstructures within the hydrogel matrix that contributes to its degradability. Drug release was not impacted by matrix degradation rate, as four different encapsulated payloads of variable hydrophobicity and molecular weight were encapsulated with the chimeric hydrogels showed comparable release rates to non-degradable alginates. These new degradable alginates could have future utility as degradable drug-eluting implants.

TABLE OF CONTENTS

LIST OF FIGURES

LIST OF SCHEMES

LIST OF ABBREVIATIONS

BSA	Bovine Serum Albumin
DCM	Dichloromethane
DMSO	Dimethyl sulfoxide
FT-IR	Fourier Transformed Infrared Spectroscopy
^{1}H-NMR	Proton Nuclear Magnetic Resonance
LWA	Low Viscosity Alginate
PLA	Polylactic Acid
TAMRA	Tetramethylrhodamine
TBA	Tetrabutylammonium
TCO	Trans-cyclooctene
UV-Vis	Ultraviolet–visible Spectroscopy

1. INTRODUCTION

Hydrogels are three-dimensional networks composed of crosslinked hydrophilic polymer chains. Because of the crosslinked structure and high-water content, hydrogels have become one of the most extensively studied materials for applications as wound dressing[1], drug-releasing implants[2], and tissue engineering scaffolds[3]. Hydrogels are mainly fabricated by the crosslinking of polymeric chains, and there are two main strategies: chemical[4] and physical crosslinking[5]. Chemically cross-linked hydrogels utilize chemical reactions to create new covalent bonds for gelation such as Diels-Alder reactions[6], Schiff base reactions[7], or Michael type additions[8]. By contrast, physical crosslinks utilize molecular interactions such as hydrogen bonding[9], crystallization[10], or ionic bonding[11].

Alginate is a naturally derived polysaccharide consisting of β-$_D$- mannuronic acid (M) and α-$_L$-guluronic acid (G) isomeric monomers. Alginate forms hydrogels rapidly in the presence of divalent cations like Ca^{2+} or Ba^{2+} as ionic crosslinkers[12]. Alginate hydrogels have been widely used in drug delivery and cell therapy because of their biocompatibility, and stable, mild crosslinking reactions[13]. However, there is no enzyme in mammals that can degrade alginate hydrogels and it usually takes months for alginate hydrogels to degrade, which can limit its in vivo utility[14]. Degradation is an important property for hydrogels as resorbable implants which can provide therapeutic function while degrading away once that function has been achieved and the implant is no longer needed. In addition, it can also enable the release of encapsulated cargos for drug delivery.

Three strategies have been developed focusing on the control of the degradation kinetics of alginate hydrogels: varying the oxidization state of alginate, using alginate lyase, and fabricating alginate hydrogels with degradable crosslinks[15]. While tunable degradation rates can be achieved by varying the oxidation state of alginate, this process can also decrease its biocompatibility[16]. Other strategies utilize degradable crosslinks that can access different degradation mechanisms like enzymatic cleavage[17], hydrolysis[18] , and external initiated degradation[19]. However, most synthetic crosslinks are not bioinert. Alginate lyase is a naturally-occurring enzyme that can digest the alginate[20]. Controlling the concentration of alginate lyase can produce degradable alginate hydrogels and promote cell release[20]. However, this enzyme can be immunogenic and increasing the concentration of alginate lyase could lower the mechanical properties of alginate hydrogels.

To overcome these limitations and as an alternative approach to fabricate degradable alginate hydrogels with tunable degradation kinetics, we hypothesized that conjugating a biocompatible and degradable biopolymer to the alginate domain chain would combine degradation and gelation properties. For our hydrolyzable and degradable material, we chose polylactic acid (PLA)since it is a widely-used synthetic polymer that is already utilized clinically uses[21]. The ester linkage on the backbone of PLA can be easily hydrolyzed by water, giving the polymer its degradation ability with a degradation rate that can be controlled by its molecular weight[22]. To synthesize our alginate-b-PLA chimera, we developed an approach to conjugate PLA to alginate utilizing an inverse

electron-demand Diels-Alder reaction. We then fabricated hydrogels from our chimeric polymers with two different strategies: doping and direct gelation. The degradation profile of our hydrogels was first measured by tracking their swelling ratios over time and characterized the mechanism of degradation by rheology , ^{1}H-NMR, and fluorescence labeling. The degradation time of the chimeric hydrogels can be tuned from days to weeks by modulating the size of alginate and PLA domain as well as by formulation. Finally, four different payloads were used to determine the potential of alginate-b-PLA hydrogels as drug delivery systems. The release studies suggested the release process of the payloads was based on diffusion mechanism and independent of the degradation process. Future studies include exploring the potential of these chimeric alginate scaffolds in tissue engineering, where scaffold degradation can influence cell proliferation and migration.

2. RESULTS

2.1 Alginate-b-PLA Synthesis

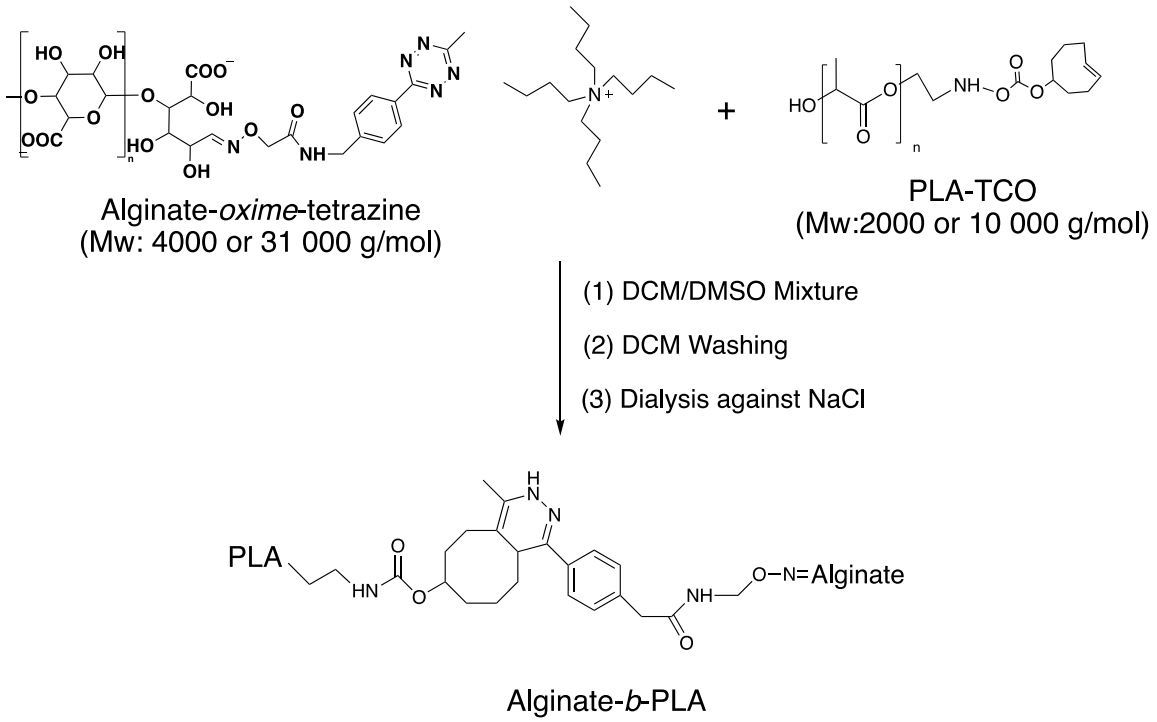

Scheme 1. Synthetic scheme of alginate-b-PLA. The ligation between alginate and PLA is mediated by inverse electron-demand Diels-Alder reaction between tetrazine and trans-cyclooctene (TCO).

To synthesize alginate-*b*-PLA diblock copolymers, alginate-tetrazine was covalently attached to PLA-TCO (**Scheme 1**). But since the solubility of these two polymers is different in organic solvent, we converted sodium alginate-tetrazine into its tetrabutylammonium (TBA) salt through ion exchange. The resulting TBA alginate-tetrazine was able to be dissolved into organic solvent and readily for reaction with PLA-TCO in DMF/DMSO. The final diblock copolymers were characterized by ^{1}H-NMR, UV-Vis spectrometer, and FT-IR.

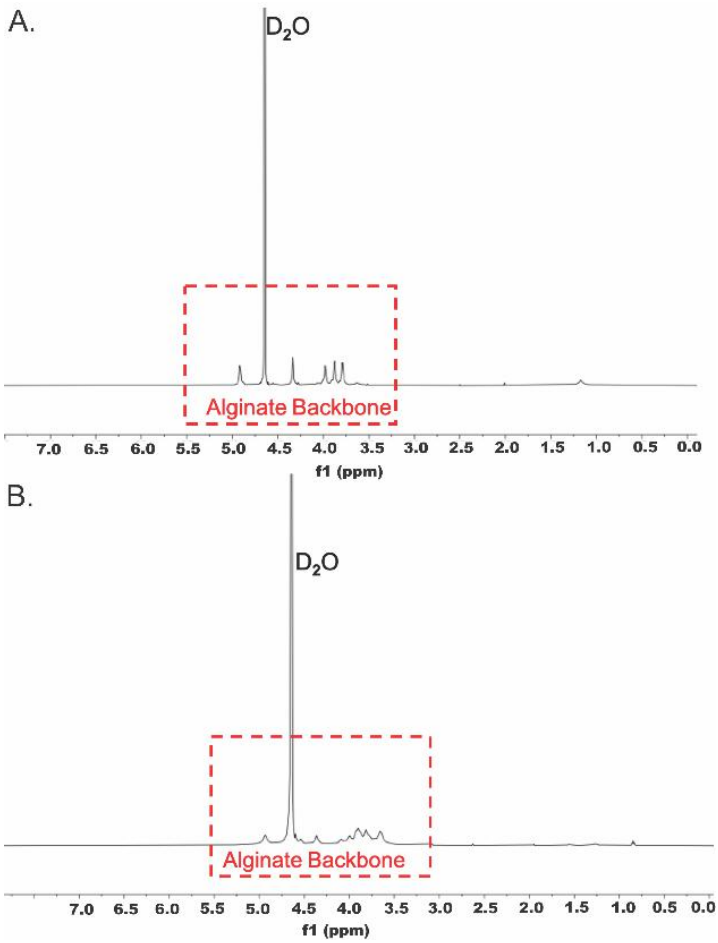

Figure 1. The 1H-NMR characterization of alginate-b-PLA: (A) alginate4K-b-PLA and (B) alginate31K-b-PLA (D2O, 500 MHz). The characteristic peak related to alginate backbone is indicated in the red box and full consumption of tetrazine and TCO was observed.

Both $Alginate_{31K}$ and $Alginate_{4K}$- based diblock copolymers were dissolving in D_2O for the ^{1}H-NMR characterization. The result shows that only peaks consistent with the alginate backbone were observed. The loss of PLA signals in D_2O indicated that the diblock copolymer exhibited potential hydrophobic aggregation in the inorganic solvent. (**Figure 1**).

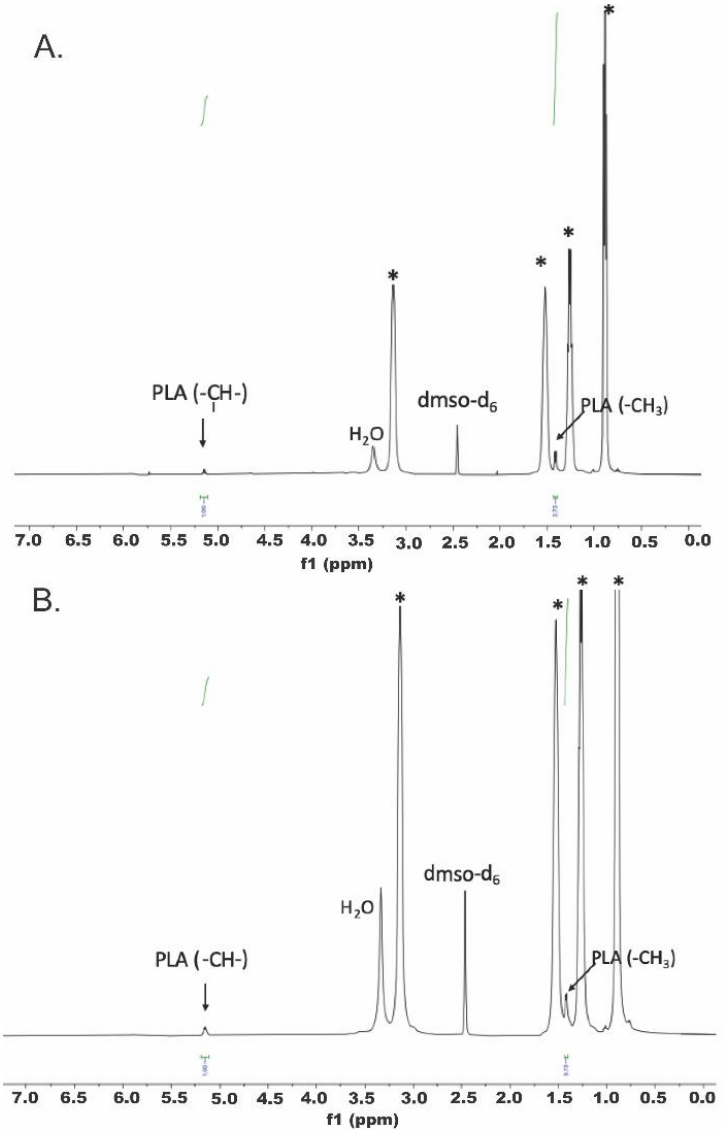

Figure 2. [1]H-NMR characterization of alginate-b-PLA: (A) alginate4K-b-PLA and (B) alginate31K-b-PLA (DMSO-d6, 500 MHz). The full consumption of tetrazine and TCO was observed. Peaks marked with * are tetrabutylammonium peaks. The designated peaks for PLA backbone were marked.

Solving the diblock copolymers in DMSO-d6, the peaks corresponding to the methyl (-CH_3) and -CH- groups of the polylactide backbone were observed at 5.10 ppm and 1.40 ppm. However, the characteristic peaks of alginate were not observed in DMSO-d6

which is consistent with the aggregation of these hydrophilic domains of alginate (**Figure 2**). Diagnostic peaks for tetrazine (7.42 and 8.23 ppm) from the alginate-tetrazine and TCO functionalities from the diblock (5.40 and 5.54 ppm) disappeared after conjugation according to ^{1}H-NMR (**Figures 2 and 3**).

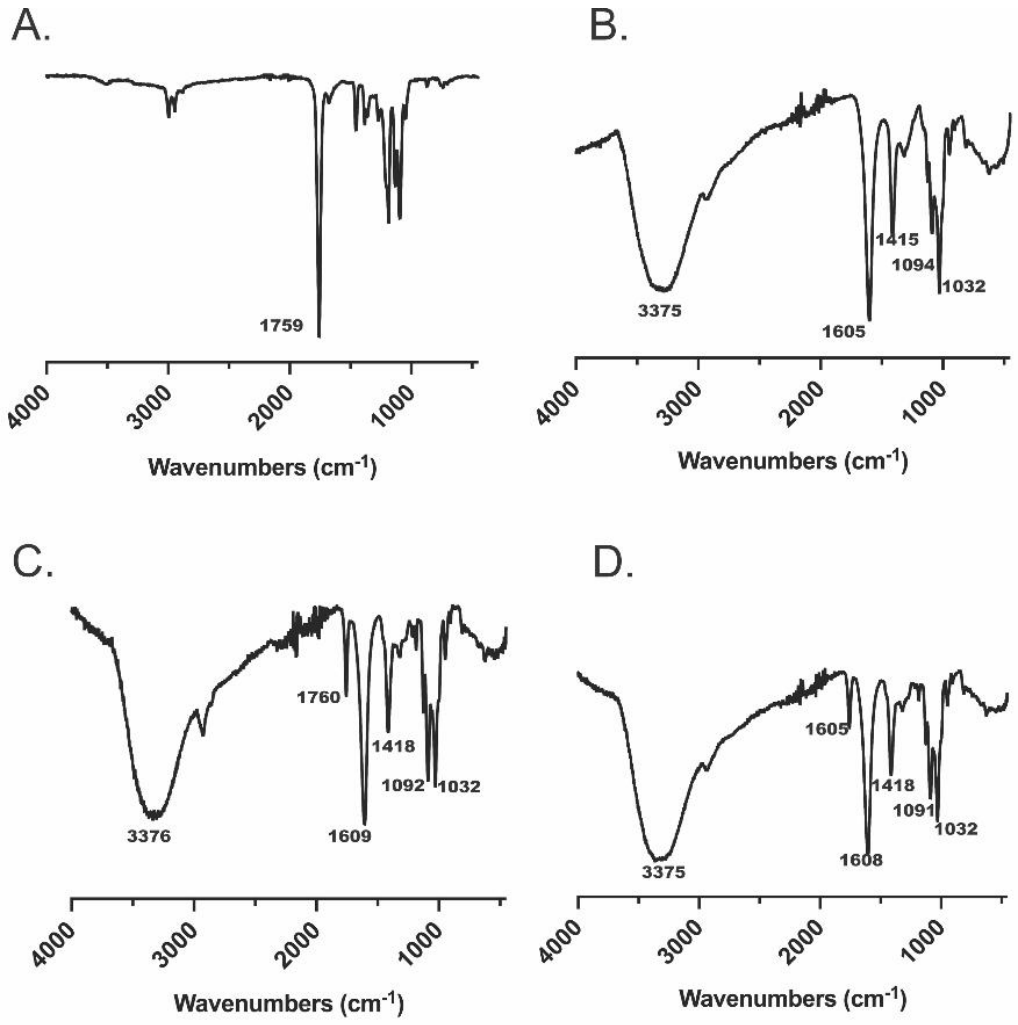

Figure 3. FTIR characterization of alginate-b-PLA diblock copolymers: (A) PLA and signature peaks were marked on the spectrum. (B) alginate-oxime-tetrazine and signature peaks were marked on the spectrum. (C) alginate4K-b-PLA and signature peaks were marked on the spectrum. (D) alginate31K-b-PLA and signature peaks were marked on the spectrum.

FTIR analysis showed the anticipated stretching vibrations of OH groups from alginate at 3375 cm^{-1}, as well as the asymmetric and symmetric stretches of the C=O from the carboxylate appeared in 1608 and 1418 cm^{-1} (**Figure 3**). The stretching of C=O of the polylactide was identified at 1752 cm^{-1} along with -CH stretching at 2961 cm^{-1}. From the UV-Vis spectrum, after conjugated with PLA-TCO, the peak related to alginate-oxime-tetrazine at 525 nm disappeared which indicated the full consumption of tetrazine (**Figure 4**). Thus, the synthesis of the alginate-*b*-PLA diblock copolymers was confirmed.

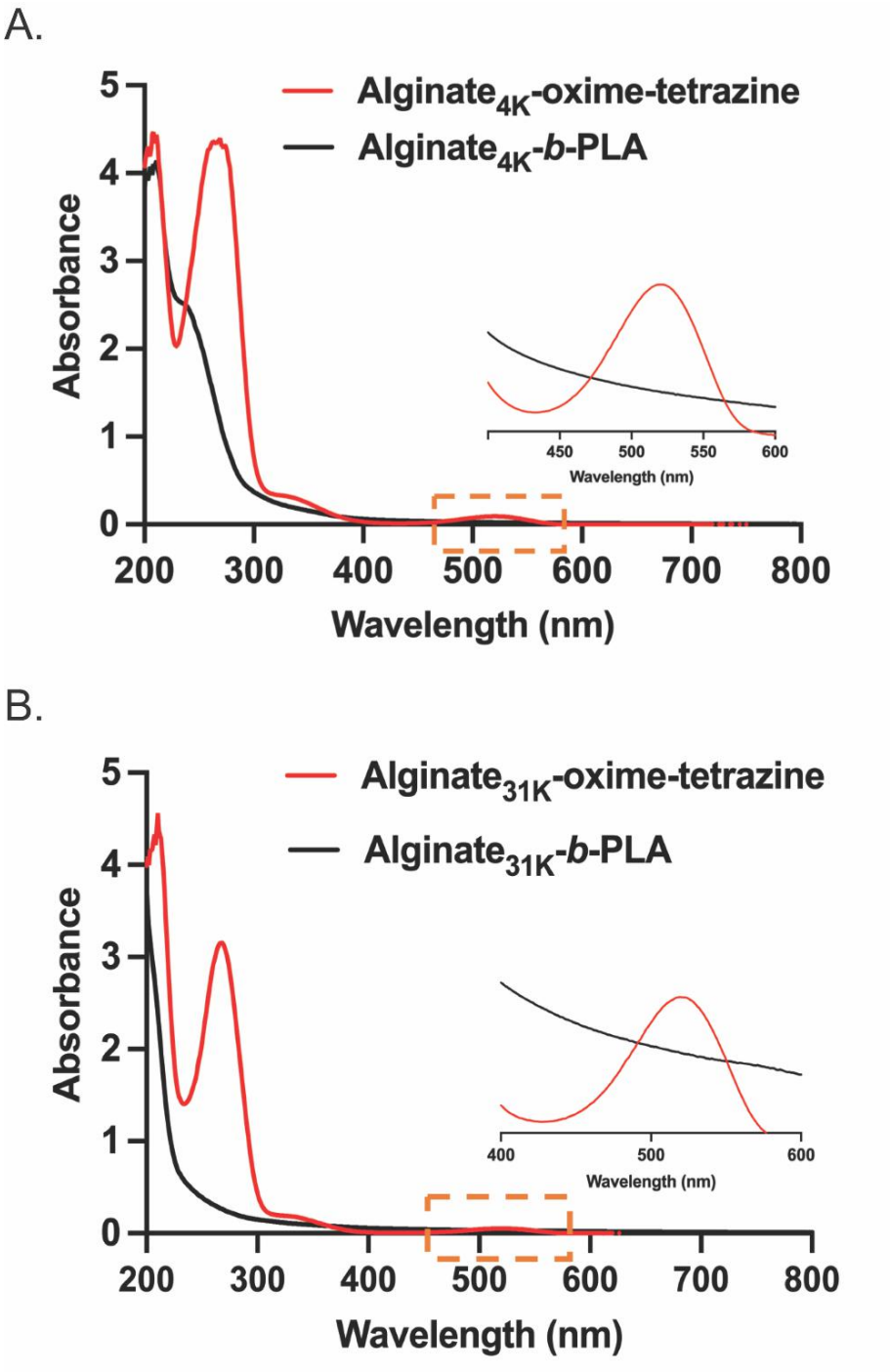

Figure 4. UV-Vis spectra of (A) alginate4K-oxime-tetrazine and alginate4K-b-PLA and (B) alginate31K-oxime-tetrazine and alginate31K-b-PLA. The full consumption of tetrazine was observed.

2.2 Fabrication and Swelling Ratio Test of Alginate-b-PLA Hydrogels

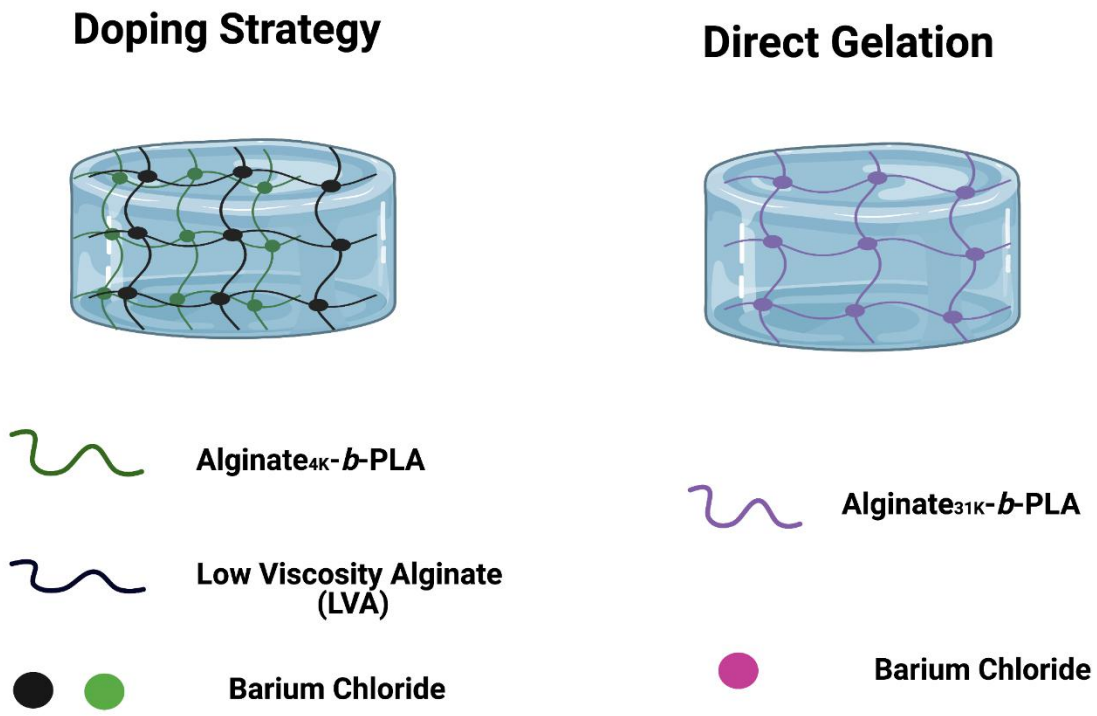

Figure 5. The graphic illustration of fabrication strategies for alginate-b-PLA chimaeras hydrogel. Doping strategy: alginate4K-b-PLA is blended with low viscosity alginate (LVA), which acts as major structural scaffold. The hydrogel is formed in the presence of barium chloride. Direct gelation: alginate31K-b-PLA diblock copolymer forms hydrogel directly in the presence of barium chloride without additional blending biomaterial.

Alginate-b-PLA diblock copolymers were then fabricated into hydrogels using ionic barium as a crosslinker. Two different strategies were implemented to fabricate alginate-*b*-PLA chimeric hydrogels (**Figure 5**). Our preliminary studies showed both alginate$_{4k}$ and alginate$_{4K}$-*b*-PLA diblock copolymers were not able to form hydrogels in the presence of barium ions due to the low molecular weight of the alginate (data not shown). Therefore, we doped alginate$_{4K}$/PLA diblock copolymers with low viscosity alginate

(LVA) in different blending ratios. Direct gelation of the chimeric polymer was possible with a larger alginate domain, which we achieved with the alginate$_{31K}$-*b*-PLA chimeras.

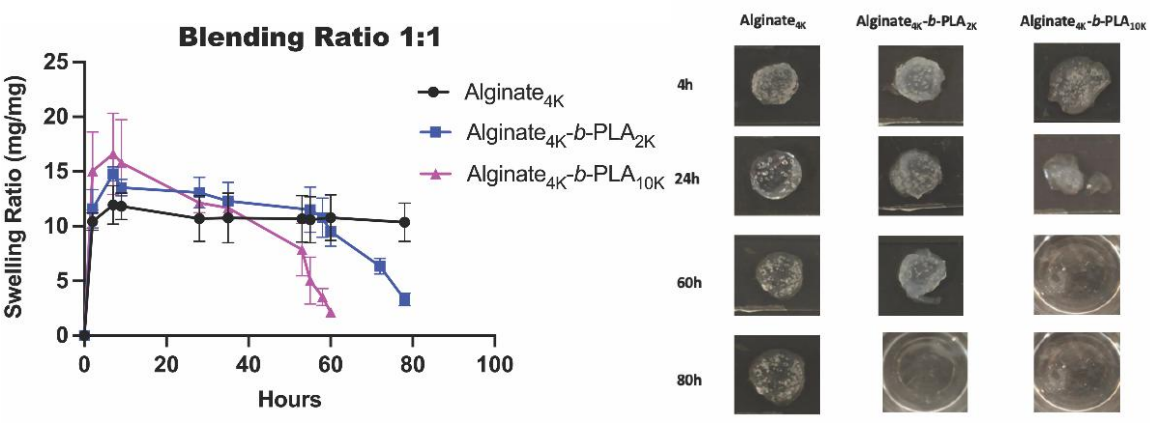

Figure 6. The degradation profile of LVA/alginate4K-b-PLA (1:1) hydrogels measured by swelling ratio and data are represented as mean +/- SD (n=3).

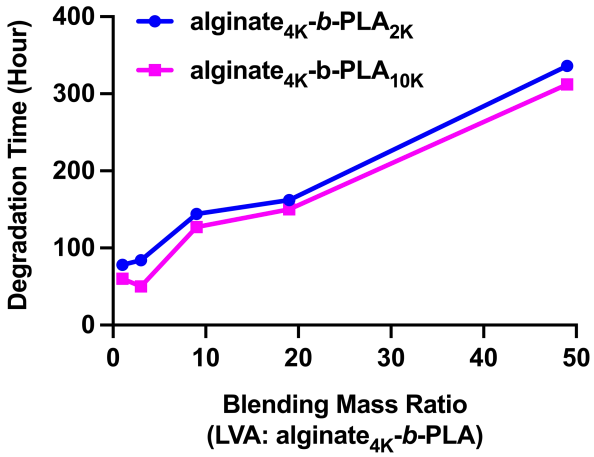

Figure 7. Degradation time of LVA/alginate4K-b-PLA hydrogels with blending ratio from 1:1 to 49:1.

The degradation process of LVA/alginate$_{4K}$-*b*-PLA blending hydrogels and alginate$_{31K}$-*b*-PLA chimeras hydrogels were tracked by measuring their swelling ratios (mass change

measurement)The lyophilized alginate hydrogel chimeras using both fabrication strategies underwent a rehydrating process for 4 hours. Then they remained at swelling equilibrium before degradation occurred. For doped hydrogels, the blending ratio between LVA and alginate$_{4K}$-*b*-PLA was varied from 1:1 to 49:1 and the degradation time of the blended hydrogels could be modulated from days to weeks (**Figure 7**). Meanwhile, the alginate$_{4K}$ hydrogel control remained relatively stable within the same time span. For LWA/alginate$_{4K}$-*b*-PLA with the blend ratio at 3:1 (**Figure 6**), the alginate$_{4K}$-*b*-PLA$_{10K}$ blended hydrogel degraded within 50 hours and alginate$_{4K}$/PLA$_{2K}$ blended hydrogel degraded within 80 hours. When increasing the blending ratio 49:1, the degradation time for alginate$_{4K}$-*b*-PLA blended hydrogels was raised to 2 weeks (**Figure 12**). Meanwhile, the degradation time difference between PLA$_{2K}$- and PLA$_{10K}$- based hydrogels indicated the influence of the size of the PLA domain on the hydrogel degradation. This difference was more pronounced at lower blending ratios. For example, the degradation time difference is 1.7 for the 3:1 blending ratio group and 1.0 for the 49:1 blending ratio. Such change can be explained by the dilution effect of LVA in the blending system. The higher the proportion of LVA in the blending system, the higher stability of the blended hydrogels. Similarly, the alginate$_{31K}$-PLA based hydrogels exhibited degradation behavior where the swelling ratio substantially decreased within 250 hrs (**Figure 8**). However, the degradation time difference between PLA$_{2K}$- and PLA$_{10K}$- based alginate$_{31K}$ hydrogels is 1.1 which showed less degradation tunability of alginate$_{31K}$-PLA comparing to the doping system.

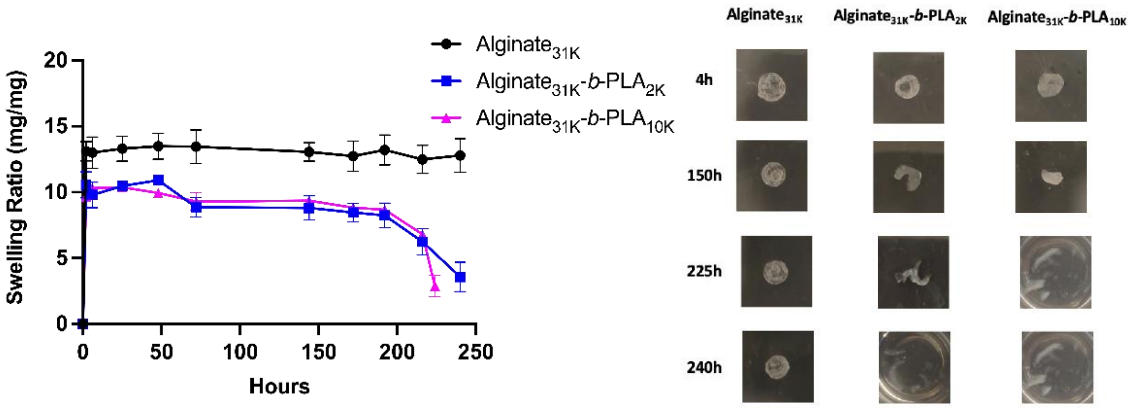

Figure 8. The degradation profile of alginate31K-b-PLA hydrogels measured by swelling ratio and data are represented as mean +/- SD (n=3).

Alginate-b-PLA diblock copolymer hydrogels also showed a higher swelling ratio compared to its corresponding alginate hydrogel control, with the exception for the LVA/alginate$_{4K}$-*b*-PLA blend (49:1). The higher swelling ratios for the copolymer-based hydrogels indicated the diblock copolymer exhibited potential hydrophobic aggregation during the gelation process, which then disrupted the crosslinking interaction between alginate and barium chloride.

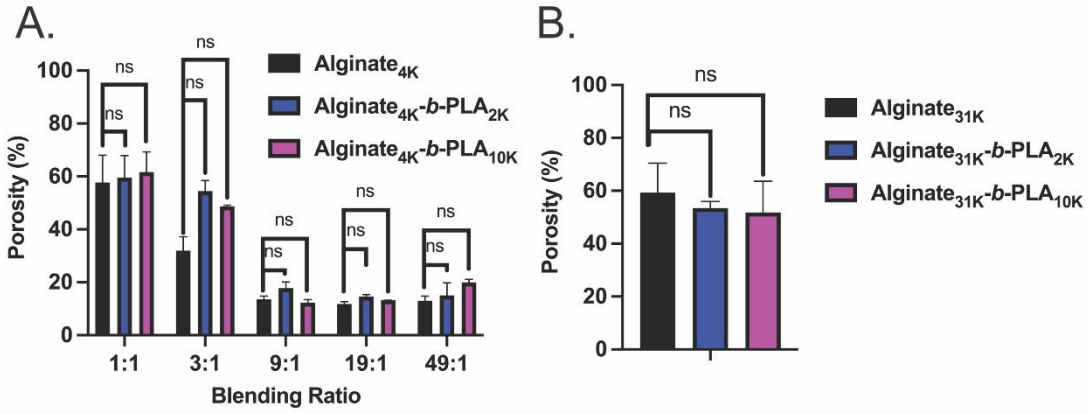

Figure 9. Porosity characterization of alginate-b-PLA alginate. (A) Porosity measurement of LVA/alginate4K-b-PLA hydrogels with blending ratio from 1:1 to 49:1. (B) Porosity measurement of alginate31K-b-PLA hydrogels.

Porosity is a fundamental parameter and hydrogel property. When the blending ratio is below or equal to 3:1, the porosity of LVA/alginate4K-PLA hydrogels is between 50-60%. When the blending ratio is larger than 3:1, the porosity is around 20%. The decline in porosity of LVA/alginate4K-b-PLA might result from the increasing weight percent of LVA, which then formed a denser network when crosslinked with barium chloride **(Figure 9)**.

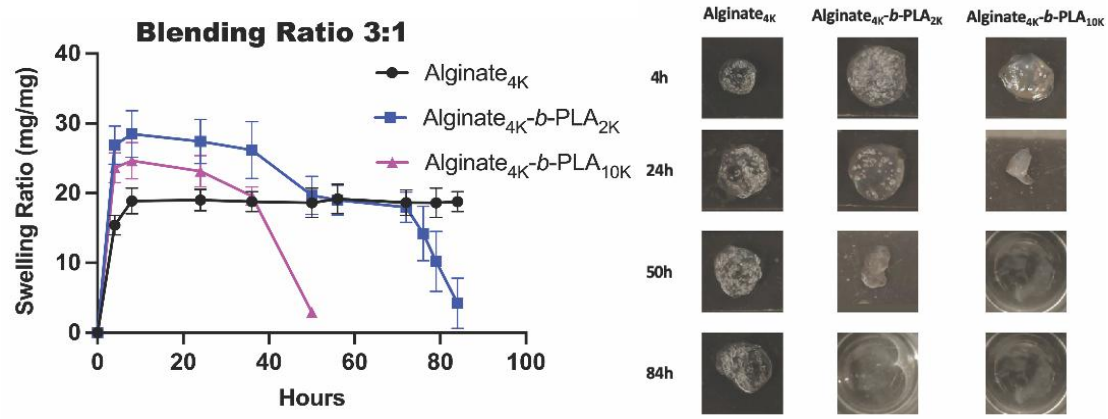

Figure 10. The degradation profile of LVA/alginate4K-b-PLA (3:1) hydrogels measured by swelling ratio and data are represented as mean +/- SD (n=3).

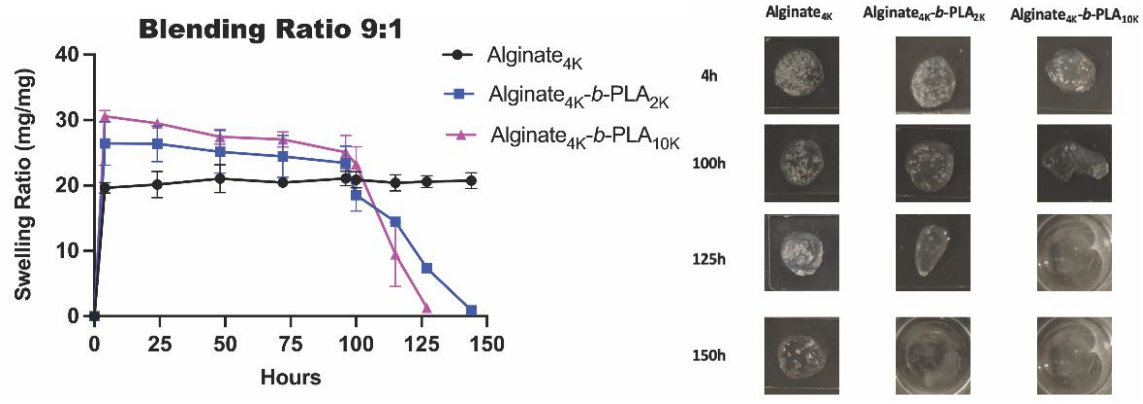

Figure 11. The degradation profile of LVA/alginate4K-b-PLA (9:1) hydrogels measured by swelling ratio and data are represented as mean +/- SD (n=3).

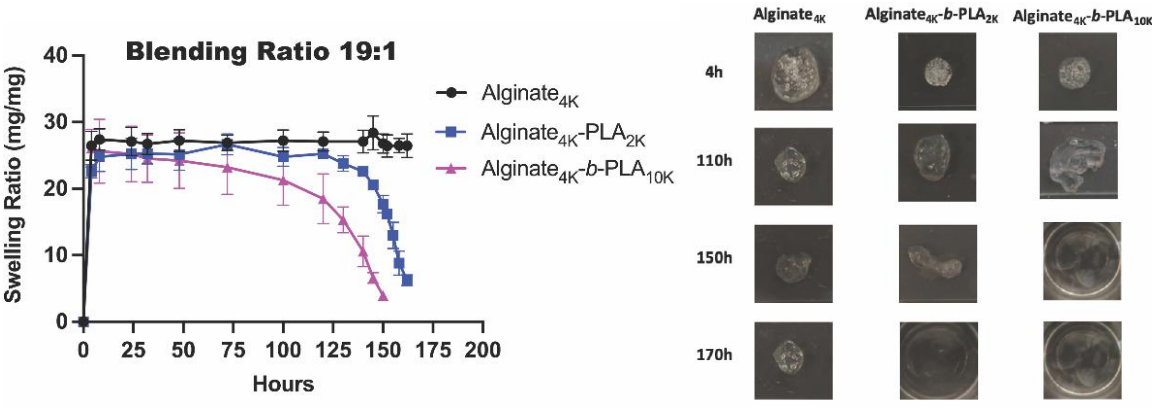

Figure 12. The degradation profile of LVA/alginate4K-b-PLA (19:1) hydrogels measured by swelling ratio and data are represented as mean +/- SD (n=3).

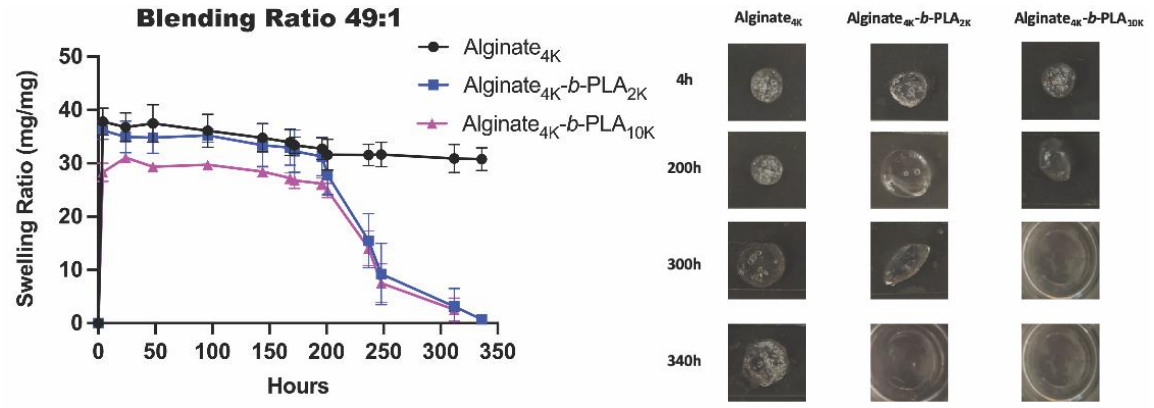

Figure 13. The degradation profile of LVA/alginate4K-b-PLA (49:1) hydrogels measured by swelling ratio and data are represented as mean +/- SD (n=3).

2.3 Degradation Mechanism Study of Alginate-b-PLA Hydrogels

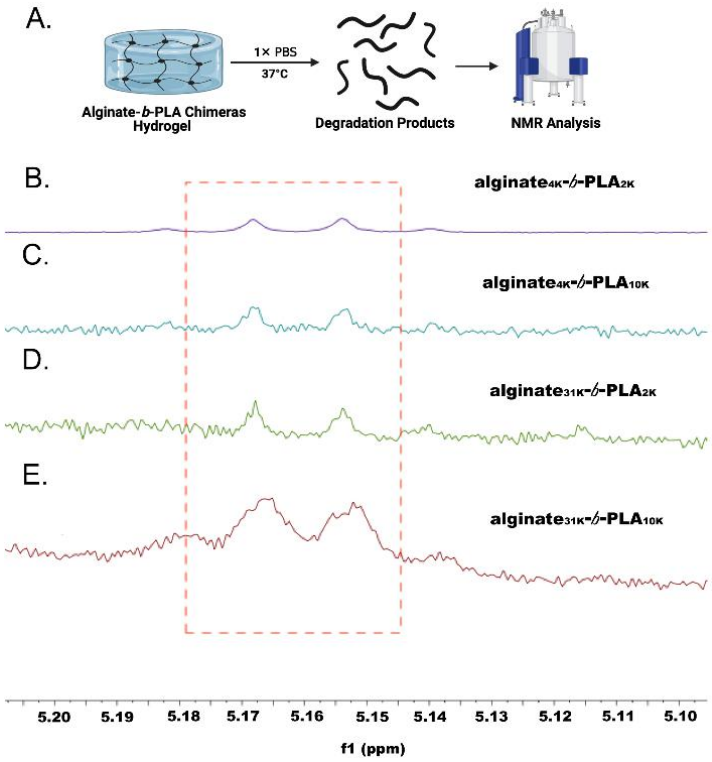

Figure 14. 1H-NMR characterizations of degradation products of alginate/PLA-based chimeras hydrogels and peak associated with PLA is marked with red box: (A) Graphic representation of experimental process (B) alginate4K-b-PLA2K (C) alginate4K-b-PLA10K (D) alginate31K-b-PLA2K (E) alginate31K-b-PLA10K.

To have a better understanding of the degradation mechanisms of alginate-b-PLA hydrogels, several experiments were carried out and with blended LVA/alginate$_{4K}$-*b*-PLA (3:1) and alginate$_{31K}$-*b*-PLA hydrogels as model systems. The final degradation products in PBS were tested by ^{1}H-NMR **(Figure 14)**. The peaks associated with free lactide were identified in both the degraded LVA/alginate$_{4K}$-*b*-PLA and alginate$_{31K}$-*b*-PLA hydrogels confirmed that the PLA domain on the alginate-b-PLA chain underwent degradation during the hydrogel degradation process.

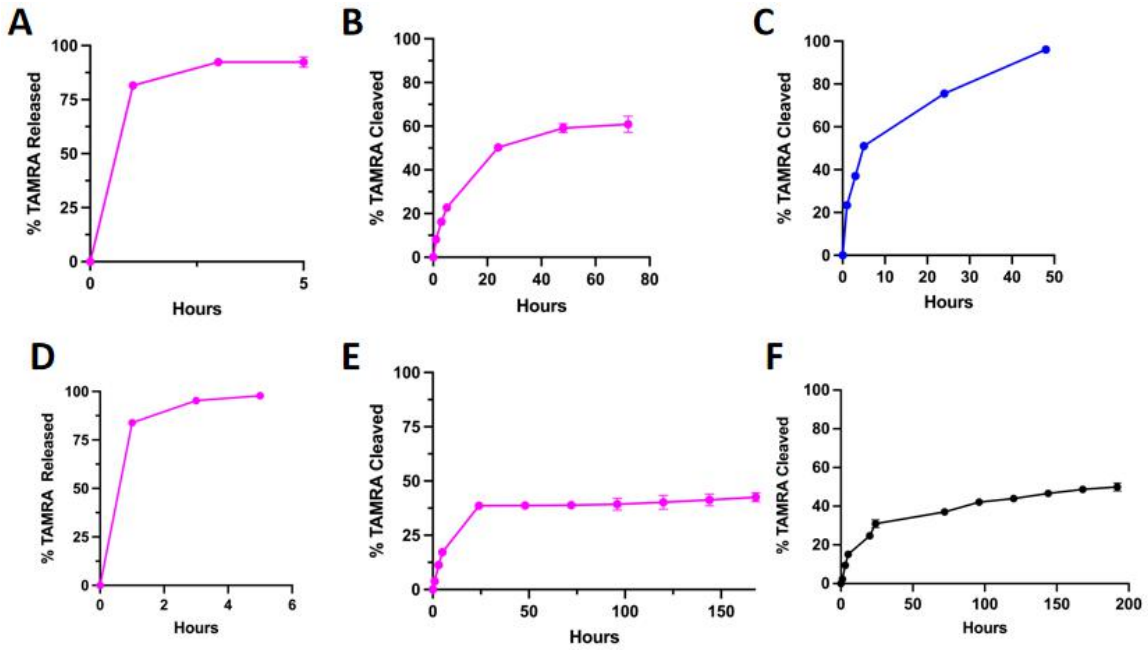

Figure 15. PLA-Dye cleavage test of alginate/PLA-based chimeras hydrogels (1 wt% TAMRA labeling diblock contained)characterized by UV-Vis: (A) LVA/alginate4K (3:1) (B) LVA/alginate4K-b-PLA2K (3:1) (C) LVA/alginate4K-b-PLA10K (3:1) (D) alginate31K (E) alginate31K-b-PLA2K (F) alginate31K-b-PLA10K. Data are represented as mean +/- SD (n=3).

In addition, TAMRA-labeled PLA was conjugated to the alginate chain and dye-labeled diblock copolymers were 1:1 blended with pure diblock copolymer for hydrogel fabrication. The PLA-Dye cleavage test showed that copolymer-based hydrogels have a slower PLA degradation rate compared to its control group of an encapsulated (but not conjugated) TAMRA. For the hydrogels with both gelation strategies, control groups released over 80% TAMRA within 6 hours (**Figure 15 A and D**). However, for the alginate$_{4k}$-PLA blended hydrogels, alginate$_{4K}$-*b*-PLA$_{2K}$ blended hydrogel released 52.3% PLA-TAMRA within 24 hours and 62.1% within 72 hours (**Figure 2.15 B**), while the alginate$_{4K}$-*b*-PLA$_{10K}$ blended hydrogel released 74.8% PLA-TAMRA within 24 hours and

96.1% within 48 hours (**Figure 15 C**). Meanwhile, the single component hydrogels of alginate$_{31K}$-*b*-PLA$_{2K}$ hydrogel released 41.2% PLA-Tamara within 24 hours (**Figure 15 E**) and the alginate$_{4K}$-*b*-PLA$_{10K}$ hydrogel released 38.5% PLA-TAMRA within 24 hours (**Figure 15 F**). Overall, the resulting amount of PLA-TAMRA released from the alginate-b-PLA based hydrogels is smaller than the control group which can be explained by the potential hydrophobic aggregation inside the hydrogel matrix.

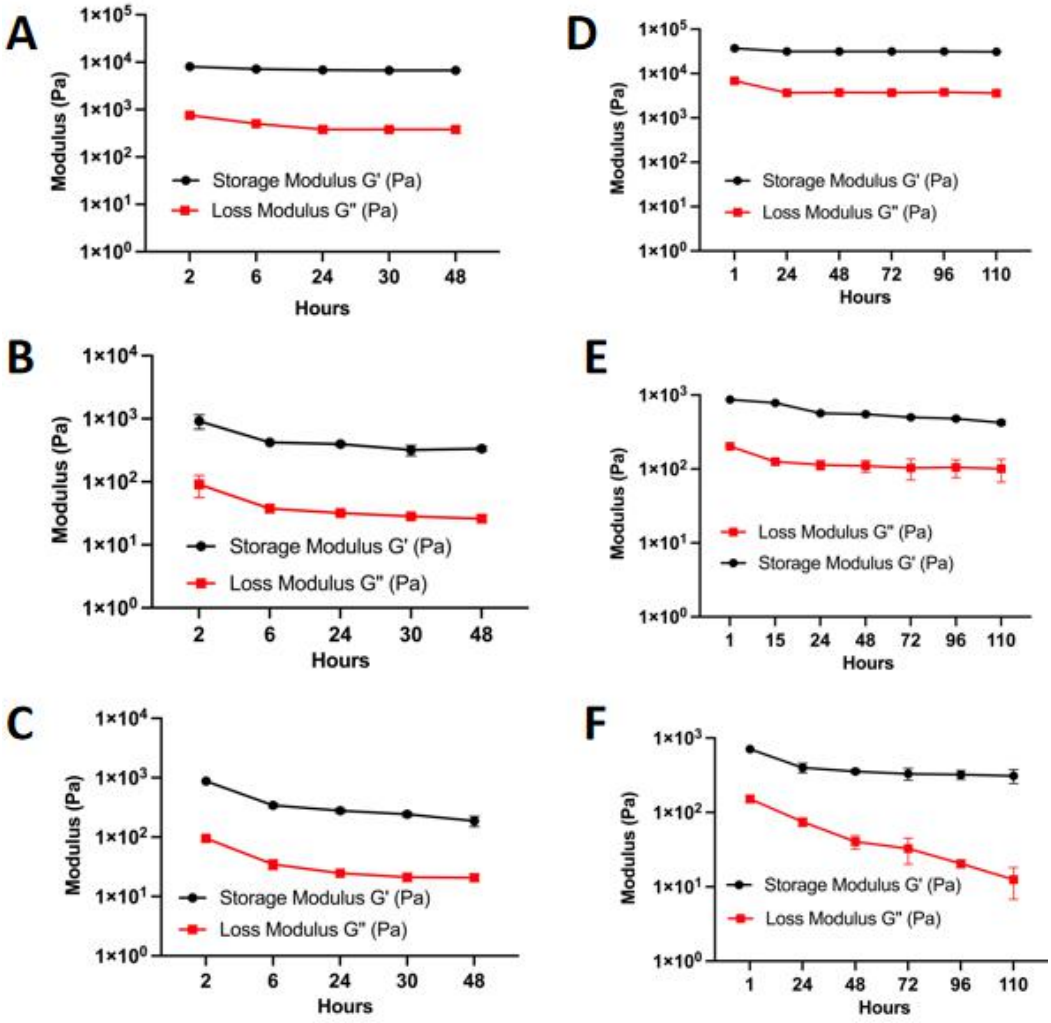

Figure 16. Degradation process of alginate/PLA-based chimeras hydrogels characterized by rheological measurements: (A) LVA/alginate4K (3:1) (B) LVA/alginate4K-b-PLA2K (3:1) (C)

LVA/alginate4K-b-PLA10K (3:1) (D) alginate31K (E) alginate31K-b-PLA2K (F) alginate31K-b-PLA10K. Data are represented as mean +/- SD (n=3).

The degradation process was then monitored by a series of rheological measurements. The storage modulus (G') of LVA/alginate$_{4K}$-b-PLA$_{2K}$ was lost by 63.6% within 24 hours compared to its initial value (**Figure 16 B**). Similarly, for LVA/alginate$_{4K}$-b-PLA$_{10K}$ hydrogel, the storage modulus (G') lost by 78% within 24 hours (**Figures 16 B**). For alginate$_{31K}$-*b*-PLA chimera hydrogels, the storage modulus (G') decreased by 51.3% and 56.3% for PLA$_{2K}$ and PLA$_{10K}$, respectively, within 24 hours (**Figure 16 E and F**). However, the swelling ratio result of both alginate$_{4k}$ and alginate$_{31k}$ based hydrogels remained relatively stable within that time span. Since the decrease in storage modulus was related to the loss of crosslinks and PLA domains, the pore size and hydrophilicity might increased during the degradation process resulting in higher water capacity. The balance between the increased amount of water contained in the hydrogels matrix and the mass loss of the crosslinks and PLA domain contributed to the swelling equilibrium in the swelling ratio profile.

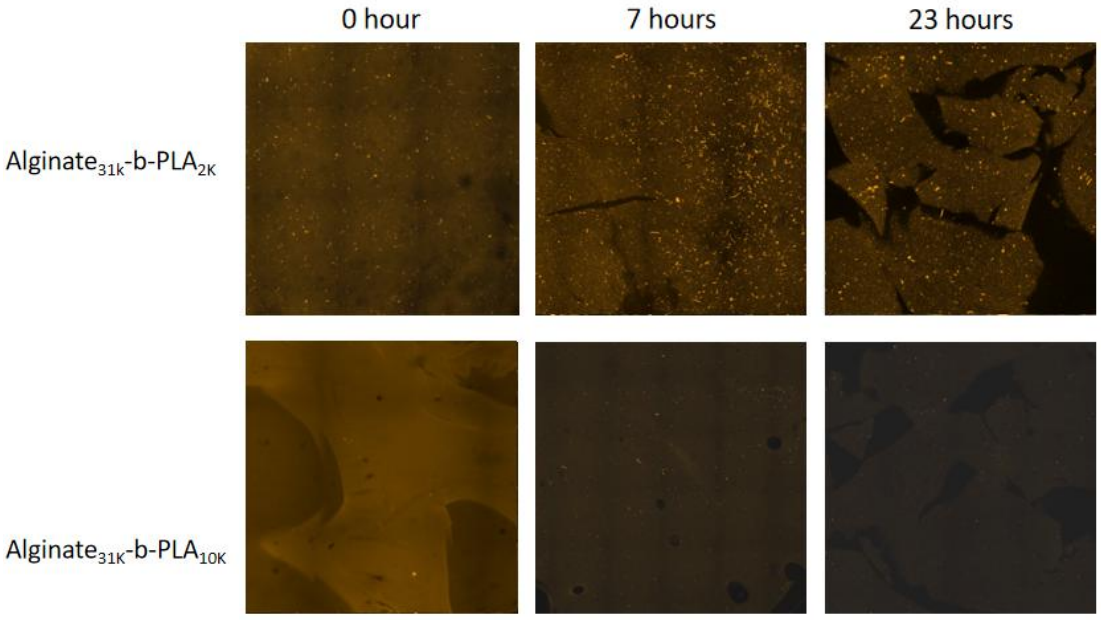

Figure 17. Degradation process of LWA/alginate4k-b-PLA (blending ratio=3:1) blended hydrogels observed by confocal microscopy (1wt% TAMRA labeling diblock contained).

We then used confocal microscopy to observe the microstructural change of the chimeric hydrogels during the degradation process. PLA aggregation is observed in both of $alginate_{4k}$ and $alginate_{31k}$ based hydrogels. (**Figures 17& Figures 18**). For the blended hydrogel chimeras, PLA_{2K}- based hydrogels showed hydrophobic aggregation in a larger size and density than the PLA_{10K}- based hydrogels **(Figures 17)**. The microstructure of $alginate_{4K}$ hydrogel chimeras suggest that the increase in hydrophobic aggregation enabled tenability of the matrix degradation rate. The amorphous part of PLA domain degraded first and caused the localized defects in the chimeric hydrogel matrix which further extended to the bulk fracture.

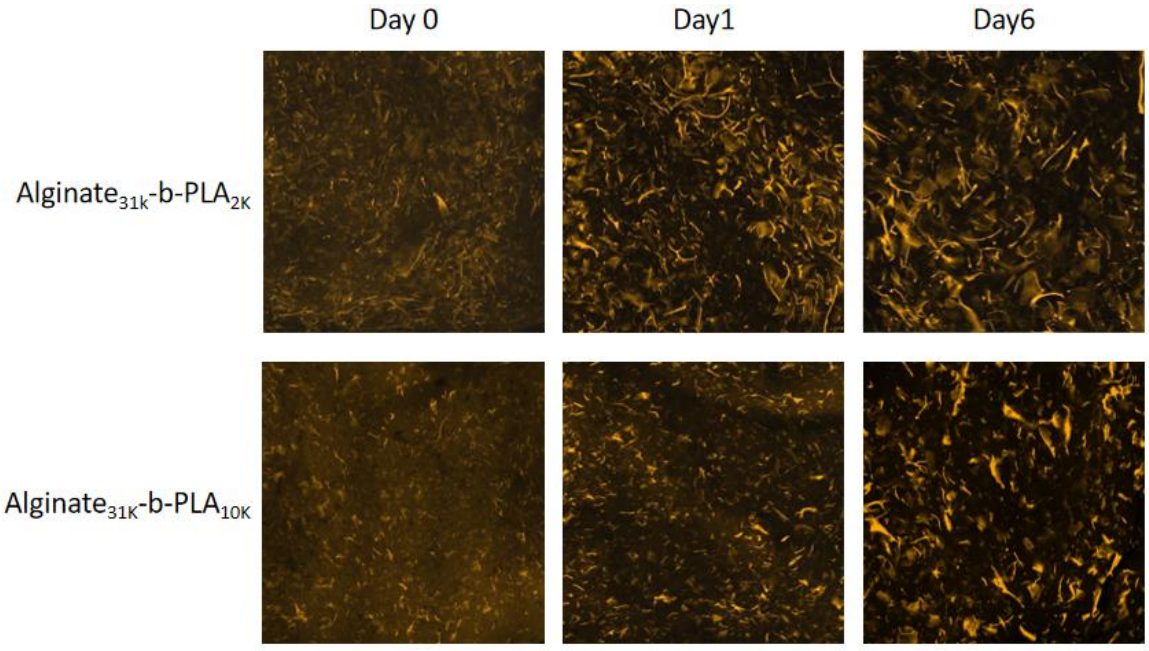

Figure 18. Hydrogel morphology and degradation of alginate31k-b-PLA hydrogels as observed by confocal microscopy after formulation with 1 wt% TAMRA labeling of the diblock polymer.

Notably, the PLA aggregation in alginate$_{31K}$-b-PLA hydrogels showed strand-like structures **(Figures 18)** compared to the blended hydrogel which presented more punctate. However, structural difference caused by the size of the PLA domain for alginate$_{31K}$-based hydrogels is not significant. The alginate$_{31K}$-PLA hydrogels showed PLA aggregation in larger size and density than the alginate$_{4K}$-PLA hydrogels, it could be explained by the dilution effect of blended hydrogels which lowered the hydrophobic interaction. Similarly, the amorphous section of alginate$_{31K}$-PLA hydrogels also degraded faster than the aggregated part which further proved that the hydrophobic aggregation enabled tenability of the matrix degradation rate.

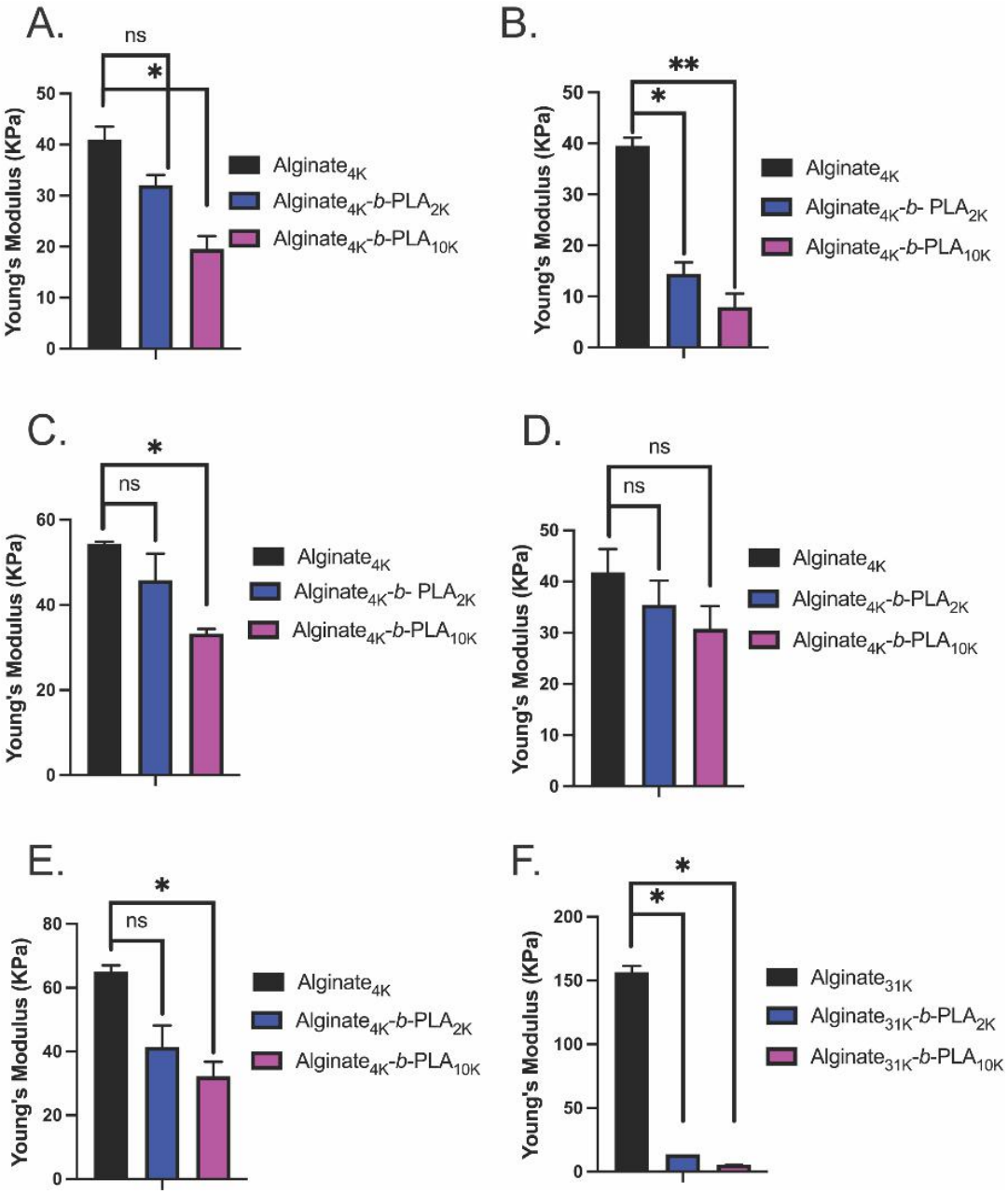

Figure 19. Mechanical characterization of alginate-b-PLA chimeras hydrogels measured by Young's modulus: (A) LVA/ alginate4K-b-PLA (1:1). (B) LVA/ alginate4K-b-PLA (3:1). (C) LVA/ alginate4K-b-PLA (9:1). (D) LVA/ alginate4K-b-PLA (19:1). (E) LVA/ alginate4K-b-PLA (49:1). (F) Alginate31K-b-PLA hydrogels. In all cases, data are represented as mean SD (n=3). For statistical analysis, ns : $p > 0.05$, *: $p < 0.05$, and ** < 0.01.

We then utilized compression testing to study the influence of PLA conjugation on the mechanical stability of our diblock hydrogels. The Young's modulus of alginate$_{31K}$ hydrogel control is 11.4- and 27.8- fold higher than alginate$_{31K}$-*b*-PLA$_{2K}$ and alginate$_{31K}$-*b*-PLA$_{10K}$ hydrogels respectively ($p<0.05$) **(Figure 19 F).** The influence of blending ranging from 1:1 to 49:1 on the Young's modulus of our blended hydrogels was determined (**Figure 19 A-E**). In general, the Young's modulus of alginate$_{4K}$ controls is 1.18-2.74 fold higher compared to PLA$_{2K}$-based hydrogels and 1.36-4.9 fold higher than PLA$_{10K}$-based system. These results showed that there is a negative correlation between the mechanical stability of chimeric hydrogels and the size of the PLA domain.

2.4 Drug Release

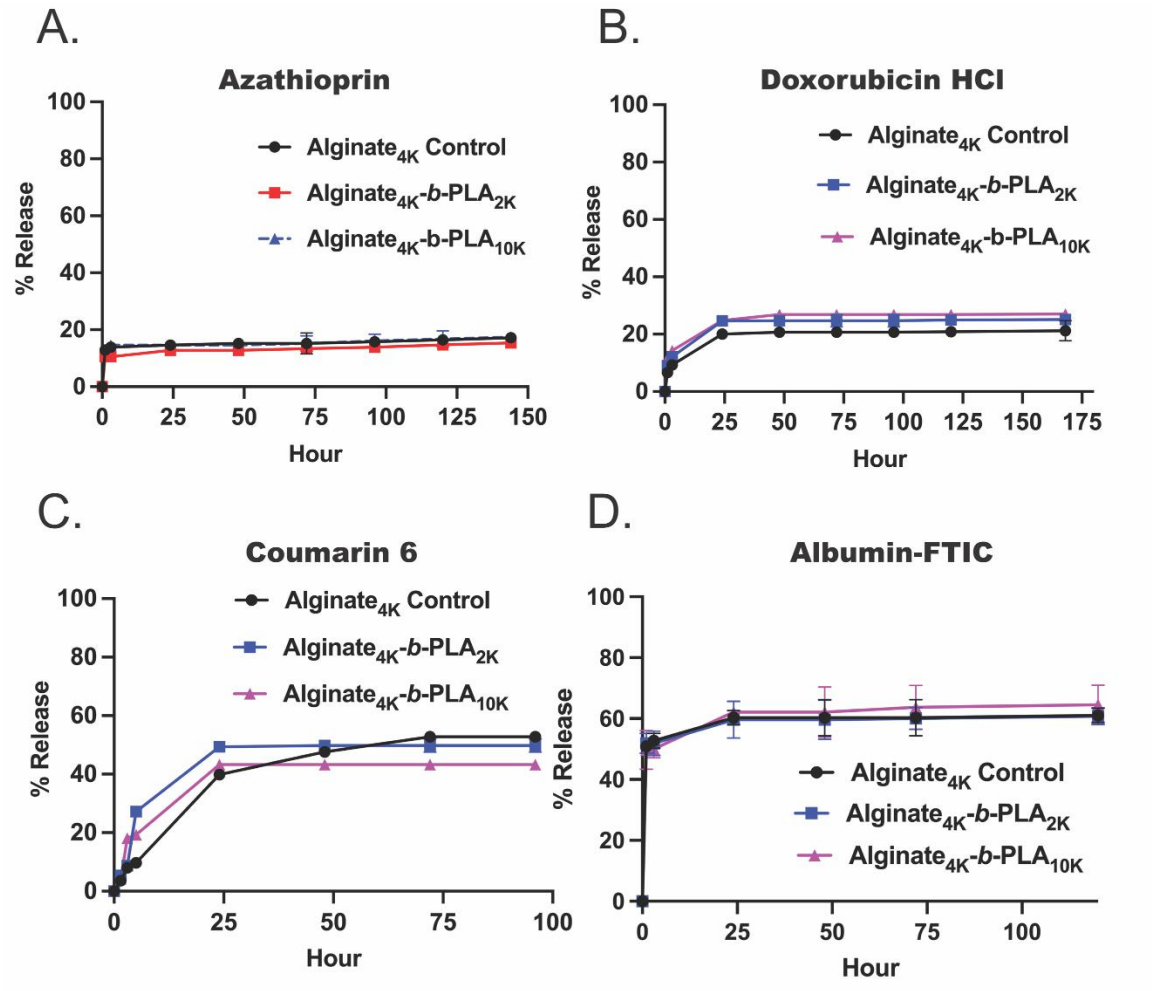

Figure 20. Payload release from LVA/alginte4K-b-PLA blended hydrogels: (A) Azathioprine (B) Doxorubicin hydrochloride (C) Coumarin 6 (D) Albumin-FTIC. Data are represented as mean +/- SD (n=3).

To investigate the capability to encapsulate and release diverse molecules for potential drug delivery application, four different payloads were encapsulated in LVA/alginate-*b*-PLA (3:1) blended hydrogels: (A) azathioprine, an immunosuppressive agent with a log P of 0.1, (B) doxorubicin hydrochloride, a chemotherapeutic drug with a log P of 0.53, (C)

coumarin 6, a fluorescent dye with a log P of 4.79, (D) Albumin-FITC, a soluble protein. In general, for each payload, there was no difference between alginate$_{4K}$ control and alginate/PLA diblock copolymer-based hydrogels in which all three hydrogel formulations released individual payloads at a consistent rate. Besides, the higher released percentage of coumarin 6 potentially resulted from the low loading level and the addition of Tween 20 (0.1%) in the 1× PBS to create the sink condition due to its high log P value. The results from the release test showed that the cargo release from the alginate-b-PLA hydrogel system was dependent more on diffusion kinetics and independent of the matrix degradation rate, likely the result of the larger mesh size of these alginate hydrogels.

3. DISCUSSION

To our knowledge, this is the first report to develop Alginate-*b*-PLA block copolymer. And the resulting diblock copolymers can be fabricated into hydrogels using two readily implemented strategies to fine-tune their degradation properties. For doped/blended hydrogels, the degradation time can be tuned from days to weeks by varying the blending ratio. For direction gelation, both PLA_{2K} and PLA_{10K}-based chimeric hydrogels can be degraded within 2 weeks. Besides, the degradation mechanism was revealed by this study. The correspondence between ^{1}H-NMR for degradation products, the PLA-TAMRA cleavage test, and the rheology-monitored degradation supported that the degradation of the chimeric hydrogels resulted from the hydrolytic degradation of the PLA domain. Although the solubility of PLA in aqueous solvents was greatly improved by conjugating it on the alginate chain, it still showed hydrophobic aggregation within the hydrogel matrix. Confocal microscopy of the internal matrix microstructure revealed that the extent of PLA aggregation imparted tunable degradation to the chimeric hydrogels. To further confirm the type of PLA aggregation, we plan to prepare XRD and DSC test for these hydrogel samples. The controlled and tunable degradation rate of the alginate-*b*-PLA hydrogel makes it an attractive degradable material for future biomedical applications and the alginate-b-PLA degradable hydrogels as an attractive platform for delivering and studying cell-material responses[23, 24] and drug payload delivery from dissolvable implants[25] in the future.

4. MATERIALS AND METHODS

4.1 Chemicals

Alginate (Pronova UPVLVG, Mn=31,000) was purchased from Novamatrix (Sandvika, Norway). Low viscosity alginate (LWA) was obtained from MP Biomedicals (OH, USA) (4-(6-methyl-1,2,4,5-tetrazin-3-yl) phenyl) methanamine was purchased from Click Chemistry Tools (AZ, USA). tBOC-aminooxy acetic acid, 1-[Bis(dimethylamino)methylene]-1H-1,2,3-triazolo[4,5-b]pyridinium3-oxide hexafluorophosphate (HATU), barium chloride (anhydrous), and solvents were purchased from Thermo Fisher Scientific (MA, USA). D-mannitol, triethylamine, hydrogen chloride solution, 4M in dioxane, was purchased from Sigma-Aldrich (MP, USA). α-amine-ω-hydroxyl poly (L-Lactide) (PLA-NH_2, MW= 2K, 10K, and 20K g/mol) was purchased from NanoSoft Polymers (NC, USA). Spectra/Por ® 7 dialysis membrane (MWCO: 2000/8000 Da) was purchased from Repligen (MA, USA).

4.2 Characterizations

^{1}H-NMR and ^{13}C NMR spectra were acquired on a Varian INOVA 500 MHz spectrometer. Infrared spectroscopy (IR) was performed on a Nicolet FT-IR with a horizontal attenuated total reflectance (ATR) adapter plate. The polymer weight of alginate was determined by GPC versus dextran standards using aqueous buffer (0.2M $NaNO_3$, 0.01 M phosphate buffer, pH 7.5) as the eluent at the rate of 0.50 ml/min through two Agilent PL aquagel columns (OH MIXED-M and OH 30, 7.5× 300 mm) at 25 °C

with a refractive index detector. UV-Visible spectra were recorded on Agilent Cary 3500.

4.3 Synthesis of Alginate-*b*-PLA

To improve the organic solubility of alginate-oxime-tetrazine, the alginate tetrabutylammonium (TBA) was formed through dialysis exchange. In a typical reaction, alginate$_{4K}$-*oxime*-tetrazine (TBA) (50 mg, 0.01 mmol) and PLA$_{10K}$-TCO (150 mg, 0.015 mmol) were dissolved in 2 ml DMSO/DCM mixture (volume ratio: 5:1). The reaction mixture was let to stir for overnight before it became colorless. The mixture was then transferred to regenerated cellulose dialysis membrane (MWCO: 8000 Da) against sodium chloride solution, followed by lyophilization. The reaction crude was then purified by dichloromethane precipitation three times to remove unreacted PLA-TCO. The precipitant was then dissolved in water and dialysis against sodium chloride solution, followed by lyophilization. The final product was a white foamy solid (130 mg, 65%). The synthesis of rest of alginate-*b*-PLA diblock copolymer followed similar protocol.

4.4 Fabrication of Alginate/PLA Diblock Copolymer-based Hydrogels

For Alginate$_{31K}$-*b*-PLA$_n$ (n=2000 and 10,000 g/mol), diblock copolymer was dissolved at 5wt% in DI water and mixed for 2 min under sonication. Samples were then centrifuged at 37°C, 4000 rpm for 20 min to remove trapped air bubble. 150 µl diblock copolymer solution was then poured into 2ml syringe and crosslinked by 150 µl 150 mM $BaCl_2$ solution / D-mannitol solution (volume ratio= 1:1) for 30 min to produce a cylindrical sample with 8mm diameter and 2mm thickness.

For Alginate$_{4K}$-*b*-PLA$_n$ (n=2000 and 10,000 g/mol), the final concentration of the LVA/Alginate$_{4K}$-*b*-PLA$_n$ blended solution was at 2 wt% and the ratio of LVA and alginate$_{4K}$-*b*-PLA was varied from 1:1. 3:1, 9:1, 19:1, and 49:1. Similarly, samples were then centrifuged at 37°C, 4000 rpm for 20 min to remove trapped air bubble. 150 µl blended polymer solution was then poured into 2ml syringe and crosslinked by 150 µl 150 mM $BaCl_2$ / D-mannitol solution (volume ratio= 1:1) for 30 min to produce a cylindrical sample with 8mm diameter and 2mm thickness.

4.5 Porosity Measurement of Alginate-*b*-PLA Chimeras Hydrogels

The solvent replacement method was used for porosity measurements. Each alginate/PLA chimera and alginate hydrogel controls were first lyophilized and dry weight (W_i) of each sample was measured. The test samples were then immersed in absolute ethanol for 3 days and weight immediately (W_f) after excess ethanol on the surface of the hydrogel was removed by Kimtech wipes. The porosity (%) was calculated as $(W_f - W_i)/(V \times \rho)) \times 100$, where V is the volume of the hydrogel disk and ρ is the density of absolute ethanol. Results were averaged on three independent runs.

4.6 Compressive Mechanical Properties of Alginate-*b*-PLA Chimeras Hydrogels

The compressive mechanical properties of alginate chimeric hydrogels were evaluated on a DHR-2 hybrid rheometer (TA Instrument, MA, USA) at room temperature. Cylindrical samples were compressed until 70% strain. During the test, the compressing rate was set as 10µm/s and stress-strain curves were recorded. The Young's modulus was calculated

from the linear part at the beginning of the stress-strain-curve regarding Hooke's law. Each measurement was performed in triplicate.

4.7 Degradation of Alginate-*b*-PLA Polymer Chimeras Hydrogels

The degradation tests were performed by incubating the pre-weighted lyophilized hydrogel samples in 5ml 1× PBS buffer at 37℃. At predetermined time intervals, the samples were removed from solution and placed on a glass slide to remove the excess water on the sample surface wiped by KimTech wipers. Each degradation study was performed in three time. The degradation profiles were assessed by measuring the swelling ratio (SR) defined by $SR = \frac{Wt-W0}{W0}$ where W_t and W_0 are the weights of the swollen samples at a particular time interval t and weights of lyophilized samples, respectively.

4.8 Hydrogel Degradation Monitored by Rheological Measurement

$Alginate_{31K}$-*b*-PLA_n and LVA/$alginate_{4K}$-b-PLA_n (3:1) were chosen model hydrogels to determine rheological properties change during degradation. Briefly, at pre-determined time points, storage modulus (G′) and loss modulus (G″) were measured with a DHR-2 hybrid rheometer (TA Instrument, MA, USA) equipped with an 8 mm diameter parallel Peltier Plate geometry at room temperature. First, viscoelastic linear regime was determined by oscillatory strain sweep test at a frequency of 10rad/s. Then, the storage modulus (G') and loss modulus (G") of hydrogels were characterized as a function of

frequency at 0.05% strain set based on viscoelastic linear regime. Each measurement was performed in triplicate.

4.9 Final Degradation Product Characterized by ^{1}H-NMR

Alginate$_{31K}$-*b*-PLA$_n$ and LVA/Alginate$_{4K}$-b-PLA$_n$ (3:1) were chosen as model hydrogels to analyze final degradation product by ^{1}H-NMR. Briefly, the degradation tests were performed by incubating the pre-weighted lyophilized hydrogel samples in 5ml 1× PBS buffer at 37℃. Towards the end of hydrogel degradation studies, 1× PBS buffers were collected. After lyophilization, the samples were washed 3 times with dichloromethane to exact degradation products and characterized by ^{1}H-NMR after vacuum drying.

4.10 Drug Release Test

For Alginate$_{4K}$-*b*-PLA$_n$ (n=2000 and 10,000 g/mol), the final concentration of the LVA/Alginate$_{4K}$-*b*-PLA$_n$ blended solution was at 2 wt% and the ratio of LVA and alginate$_{4K}$-*b*-PLA was 3:1. For azathioprine, doxorubicin hydrochloride and albumin-FTIC, 300 μg each payload was mixed with 150 μl blended polymer solution before pouring into 2ml syringe and crosslinked by 150 μl 150 mM $BaCl_2$ / D-mannitol solution (volume ratio= 1:1) for 30 min to produce a cylindrical sample with 8mm diameter and 2mm thickness. For coumarin 6, 30 μg was encapsulated into the hydrogel. The samples were then immersed in 8ml 1× PBS buffer at 37℃. At predetermined time intervals, 5ml 1× PBS buffer was removed and replenished with equivalent fresh medium to maintain a sink condition. For coumarin 6, 1× PBS buffer containing 0.1% Tween 80 was used due to its high hydrophobicity. The amount of the released payload was then analyzed for

UV-Vis absorbance using HPLC or microplate reader after lyophilization (276 nm for azathioprine, 480 nm for doxorubicin hydrochloride, 450 nm for coumarin 6, and 490 nm for albumin-FTIC). Each degradation study was performed in three times.

4.11 PLA-TAMRA Cleavage Test

For Alginate$_{4K}$-*b*-PLA$_n$ (n=2000 and 10,000 g/mol), the final concentration of the LVA/Alginate$_{4K}$-*b*-PLA$_n$/Alginate$_{4K}$-*b*-PLA$_n$-TAMRA blended solution was at 2 wt%; the ratio of LVA and alginate$_{4K}$-*b*-PLA was 3:1 and the ratio of Alginate$_{4K}$-*b*-PLA$_n$ and Alginate$_{4K}$-*b*-PLA$_n$-TAMRA was 1:1. Then 150 µl polymer solution before pouring into 2ml syringe and crosslinked by 150 µl 150 mM $BaCl_2$ / D-mannitol solution (volume ratio= 1:1) for 30 min to produce a cylindrical sample with 8mm diameter and 2mm thickness. The samples were then immersed in 8ml 1 × PBS buffer at 37℃. At predetermined time intervals, 5ml 1 × PBS buffer was removed and replenished with equivalent fresh medium to maintain a sink condition. The amount of the released PLA-TAMRA was then analyzed for UV-Vis absorbance using HPLC or microplate reader after lyophilization. Each degradation study was performed in three times.

4.12 Microscopic Confocal Test

The samples were prepared as described above (4.11) and cut into 5mm thickness slice. The samples were then immersed in 8ml 1× PBS buffer at 37℃. The samples were then removed from PBS solution at predetermined time intervals. A Olympus FV3000, with an Olympus 60 lens was used.

BIBLIOGRAPHY

1. Balakrishnan, B., Mohanty, M., Umashankar, P.R. and Jayakrishnan, A., 2005. Evaluation of an in situ forming hydrogel wound dressing based on oxidized alginate and gelatin. Biomaterials, 26(32), pp. 6335-6342.

2. Ashley, G.W., Henise, J., Reid, R. and Santi, D.V., 2013. Hydrogel drug delivery system with predictable and tunable drug release and degradation rates. Proceedings of the National Academy of Sciences of the United States of America, 110(6), pp. 2318-2323.

3. Holland, T.A., Bodde, E.W.H., Cuijpers, V.M.J.I., Baggett, L.S., Tabata, Y., Mikos, A.G. and Jansen, J.A., 2007. Degradable hydrogel scaffolds for in vivo delivery of single and dual growth factors in cartilage repair. Osteoarthritis and Cartilage, 15(2), pp. 187-197.

4. Jeon, O., Bouhadir, K.H., Mansour, J.M. and Alsberg, E., 2009. Photocrosslinked alginate hydrogels with tunable biodegradation rates and mechanical properties. Biomaterials, 30(14), pp. 2724-2734. https://doi.org/10.1016/j.biomaterials.2009.01.034

5. Eiselt, P., Yeh, J., Latvala, R.K., Shea, L.D. and Mooney, D.J., 2000. Porous carriers for biomedical applications based on alginate hydrogels. Biomaterials, 21(19), pp. 1921-1927.

6. Nimmo, C.M., Owen, S.C. and Shoichet, M.S., 2011. Diels-Alder click cross-linked hyaluronic acid hydrogels for tissue engineering. Biomacromolecules, 12(3), pp. 824-830.

7. Wu, X., He, C., Wu, Y. and Chen, X., 2016. Synergistic therapeutic effects of Schiff's base cross-linked injectable hydrogels for local co-delivery of metformin and 5-fluorouracil in a mouse colon carcinoma model. Biomaterials, 75, pp. 148-162.

8. Lutolf, M.P. and Hubbell, J.A., 2003. Synthesis and physicochemical characterization of end-linked poly (ethylene glycol)-co-peptide hydrogels formed by Michael-type addition. Biomacromolecules, 4(3), pp. 713-722.

9. Shao, C., Chang, H., Wang, M., Xu, F. and Yang, J., 2017. High-strength, tough, and self-healing nanocomposite physical hydrogels based on the synergistic effects of dynamic hydrogen bond and dual coordination bonds. ACS Applied Materials & Interfaces, 9(34), pp. 28305-28318.

10. Stenekes, R.J.H., Talsma, H. and Hennink, W.E., 2001. Formation of dextran hydrogels by crystallization. Biomaterials, 22(13), pp. 1891-1898.

11. Park, H., Kang, S.W., Kim, B.S., Mooney, D.J. and Lee, K.Y., 2009. Shear‐reversibly crosslinked alginate hydrogels for tissue engineering. Macromolecular Bioscience, 9(9), pp. 895-901.

12. Li, G., Zhang, G., Sun, R. and Ching-Ping, W., 2017. Mechanical strengthened alginate/polyacrylamide hydrogel crosslinked by barium and ferric dual ions. Journal of Materials Science, 52(14), pp. 8538-8545.

13. Lee, K.Y. and Mooney, D.J., 2012. Alginate: properties and biomedical applications. Progress in Polymer Science, 37(1), pp. 106-126.

14. Jeon, O., Alt, D.S., Ahmed, S.M. and Alsberg, E., 2012. The effect of oxidation on the degradation of photocrosslinkable alginate hydrogels. Biomaterials, 33(13), pp. 3503-3514.

15. Boontheekul, T., Kong, H.J. and Mooney, D.J., 2005. Controlling alginate gel degradation utilizing partial oxidation and bimodal molecular weight distribution. Biomaterials, 26(15), pp. 2455-2465.

16. Nguyen, T.P. and Lee, B.T., 2012. Fabrication of oxidized alginate-gelatin-BCP hydrogels and evaluation of the microstructure, material properties and biocompatibility for bone tissue regeneration. Journal of Biomaterials Applications, 27(3), pp. 311-321.

17. Wang, Y., Han, F., Hu, B., Li, J. and Yu, W., 2006. In vivo prebiotic properties of alginate oligosaccharides prepared through enzymatic hydrolysis of alginate. Nutrition Research, 26(11), pp. 597-603.

18. Lueckgen, A., Garske, D.S., Ellinghaus, A., Desai, R.M., Stafford, A.G., Mooney, D.J., Duda, G.N. and Cipitria, A., 2018. Hydrolytically-degradable click-crosslinked alginate hydrogels. Biomaterials, 181, pp. 189-198.

19. Ifkovits, J.L. and Burdick, J.A., 2007. Photopolymerizable and degradable biomaterials for tissue engineering applications. Tissue Engineering, 13(10), pp. 2369-2385.

20. Chou, A.I., Akintoye, S.O. and Nicoll, S.B., 2009. Photo-crosslinked alginate hydrogels support enhanced matrix accumulation by nucleus pulposus cells in vivo. Osteoarthritis and Cartilage, 17(10), pp. 1377-1384.

21. Campbell, K.T., Stilhano, R.S. and Silva, E.A., 2018. Enzymatically degradable alginate hydrogel systems to deliver endothelial progenitor cells for potential revasculature applications. Biomaterials, 179, pp. 109-121.

22. DeStefano, V., Khan, S. and Tabada, A., 2020. Applications of PLA in modern medicine. Engineered Regeneration, 1, pp. 76-87.

23. Wang, D.K., Varanasi, S., Fredericks, P.M., Hill, D.J., Symons, A.L., Whittaker, A.K. and Rasoul, F., 2013. FT‐IR characterization and hydrolysis of PLA‐PEG‐PLA based copolyester hydrogels with short PLA segments and a cytocompatibility study. Journal of Polymer Science Part A: Polymer Chemistry, 51(24), pp. 5163-5176.

24. Huynh, V., Jesmer, A.H., Shoaib, M.M. and Wylie, R.G., 2018. Influence of hydrophobic cross-linkers on carboxybetaine copolymer stimuli response and hydrogel biological properties. Langmuir, 35(5), pp. 1631-1641.

25. Pillai, J.J., Thulasidasan, A.K.T., Anto, R.J., Chithralekha, D.N., Narayanan, A. and Kumar, G.S.V., 2014. Folic acid conjugated cross-linked acrylic polymer (FA-CLAP) hydrogel for site specific delivery of hydrophobic drugs to cancer cells. Journal of Nanobiotechnology, 12(1), pp. 1-9.

CURRICULUM VITAE